

Figure S1. Mutants in genes related to ergosterol biosynthesis display defects in iron regulon activation upon iron deficiency. (A) Wild-type (WT, BY4741), *erg4Δ*, *erg2Δ*, *erg3Δ* and *erg5Δ* were cultivated as described in Figure 2A. The mRNA levels of *FET3*, *FTR1*, *ARN2*, *FIT3* and *FIT1*, normalized to *PGK1* mRNA, were determined by RT-qPCR and represented in relation to wild-type strain in -Fe. (B-D) The mRNA levels of *CTH2*, *FRE4* and *AFT1*, normalized to *ACT1* mRNA, were determined in wild-type (WT, W303), *upc2Δ*, *ecm22Δ* and *upc2Δecm22Δ* cells of Figure 2B-D and represented in relation to wild-type strain in +Fe. In all cases, data show average and SD of 3 biologically independent experiments. Different letters indicate statistically significant differences between each strain for a specific mRNA (p value < 0.05).

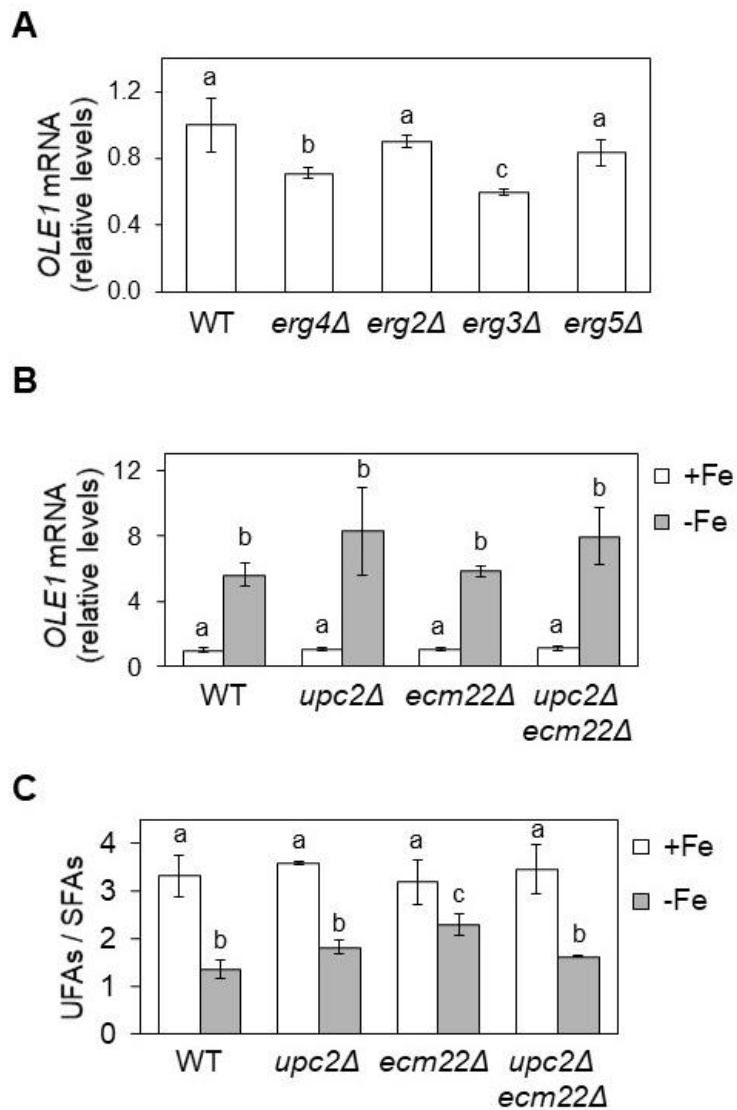


Figure S2. The limitation of iron regulon activation in cells with defects in ergosterol biosynthesis is not due to a decrease in UFA synthesis. (A) Levels of *OLE1* mRNA, normalized with *PGK1*, in wild-type (WT, BY4741), *erg4Δ*, *erg2Δ*, *erg3Δ* and *erg5Δ* cells of Figures 1 and 3A. (B) Levels of *OLE1* mRNA, normalized with *ACT1*, in wild-type (WT, W303), *upc2Δ*, *ecm22Δ* and *upc2Δecm22Δ* cells of Figure 2B-D. In both cases, data represent the average and SD of 3 biologically independent experiments, relative to WT cells in -Fe (A) or +Fe conditions (B). (C) Wild-type (WT, W303), *upc2Δ*, *ecm22Δ* and *upc2Δecm22Δ* cells were cultivated as described in Figure 4. UFA and SFA percentages were determined as described in Material and Methods, and the average and standard deviation in UFA/SFA ratio of four biologically independent experiments was represented. Different letters represent significant differences (p value < 0.05).

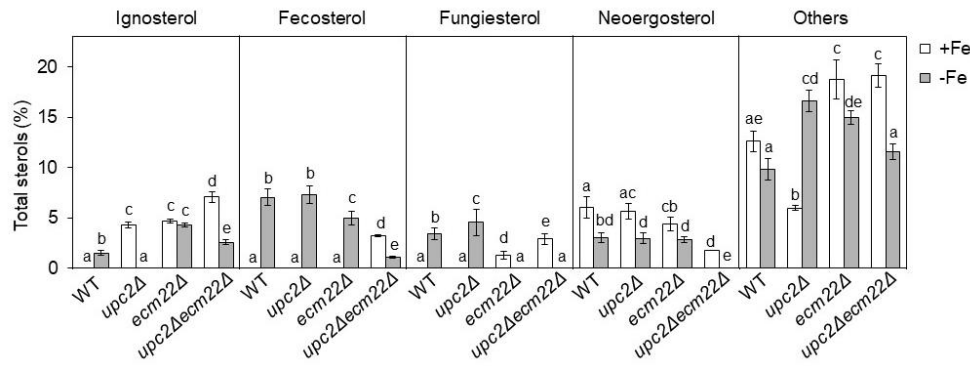


Figure S3. Iron deficiency modifies the sterols profile of *Upc2/Ecm22* mutants. Relative levels of sterol intermediates, including ignosterol, fecosterol, fungisterol, neoergosterol and others, were determined in cells from Figure 4. Data were analyzed and represented as in Figure 5.

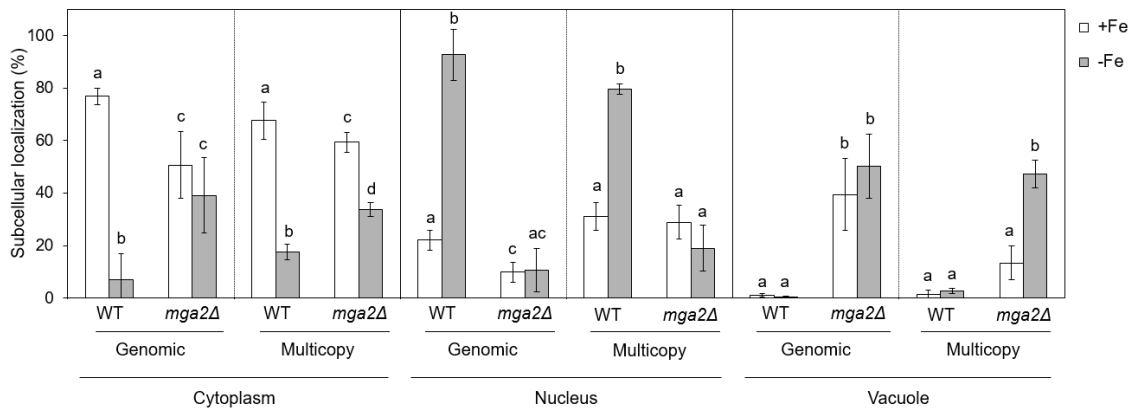


Figure S4. The localization of Aft1 protein is altered in *mga2* Δ mutants grown in iron-sufficient conditions. Wild-type (WT, BY4741) and *mga2* Δ (SPY824) cells expressing a genomic Aft1-GFP or a plasmid-expressed GFP-Aft1 (JK1346, pRS426-GFP-AFT1) were cultivated at 30 °C for 6 hours to exponential phase in SC or in SC-Ura, respectively, without (+Fe) or with 100 μ M BPS (-Fe). Quantitative analysis of Aft1 protein localization patterns were performed as described in Figure 7. Different letters represent significant differences within the same box (p value < 0.05).

Table S1. Description and source of yeast strains and plasmids used in this work.

Strain/Plasmid	Description	Source
<i>Strains</i>		
BY4741	MAT α <i>his3Δ1 leu2Δ0 met15Δ0 ura3Δ0</i>	Invitrogen
SPY1161	BY4741 <i>erg2::KanMX4</i>	Invitrogen
SPY1162	BY4741 <i>erg3::KanMX4</i>	Invitrogen
SPY1163	BY4741 <i>erg4::KanMX4</i>	Invitrogen
SPY1164	BY4741 <i>erg5::KanMX4</i>	Invitrogen
W303-1a	MAT α <i>ade2-1 leu2-3,112 his3-1 ura3-52 trp1-100 can1-100</i>	[1]
JRY7179	W303-1a <i>upc2::HIS3</i>	[1]
JRY7180	W303-1a <i>ecm22::TRP1</i>	[1]
JRY7181	W303-1a <i>ecm22::TRP1 upc2::HIS3</i>	[1]
SPY824	BY4741 <i>mga2::KanMX4</i>	Invitrogen
SPY1212	BY4741 <i>AFT1-GFP::His3MX6</i>	This study
SPY1213	BY4741 <i>mga2::KanMX4 AFT1-GFP::His3MX6</i>	This study
<i>Plasmids</i>		
P _{FET3} -lacZ	CEN <i>URA3 P_{FET3}-lacZ</i>	J. Kaplan
pSP441	CEN <i>URA3 P_{CYC1-FcRE}-lacZ</i>	[2]
JK1346	2 μ m <i>URA3 GFP-AFT1</i>	J. Kaplan
pRS416	CEN <i>URA3</i>	M. Funk
pRS416-AFT1-1 ^{up} -12HA	CEN <i>URA3 AFT1-1^{up}(C291F)-12HA</i>	[3]
pNEV-N	2 μ m <i>URA3</i>	[4]
pNEV-DAN1	pNEV-N <i>P_{PMA1}-AUS1</i>	[4]

YEp13	2 μ m LEU2	[4]
YEp13-AUS1	YEp13 P_{PMA1} -AUS1	[4]
pFA6a-GFP(S65T)-His3MX6	GFP(S65T)- T_{ADH1} -His3MX6	[5]

[1] Vik, A., & Rine, J. (2001). Upc2p and Ecm22p, dual regulators of sterol biosynthesis in *Saccharomyces cerevisiae*. *Mol Cell Biol*, 21(19), 6395-6405. doi:10.1128/MCB.21.19.6395-6405.2001

[2] Puig, S., Askeland, E., & Thiele, D. J. (2005). Coordinated remodeling of cellular metabolism during iron deficiency through targeted mRNA degradation. *Cell*, 120(1), 99-110. doi:10.1016/j.cell.2004.11.032

[3] Ueta, R., Fujiwara, N., Iwai, K., & Yamaguchi-Iwai, Y. (2012). Iron-induced dissociation of the Aft1p transcriptional regulator from target gene promoters is an initial event in iron-dependent gene suppression. *Mol Cell Biol*, 32(24), 4998-5008. doi:10.1128/MCB.00726-12

[4] Alimardani, P., Regnacq, M., Moreau-Vauzelle, C., Ferreira, T., Rossignol, T., Blondin, B., & Berges, T. (2004). SUT1-promoted sterol uptake involves the ABC transporter Aus1 and the mannoprotein Dan1 whose synergistic action is sufficient for this process. *Biochem J*, 381(Pt 1), 195-202. doi:10.1042/BJ20040297

[5] Longfane, M. S., McKenzie, A., 3rd, Demarini, D. J., Shah, N. G., Wach, A., Brachat, A., Philippson, P., & Pringle, J. R. (1998). Additional modules for versatile and economical PCR-based gene deletion and modification in *Saccharomyces cerevisiae*. *Yeast*, 14(10), 953-961. doi:10.1002/(SICI)1097-0061(199807)14:10<953::AID-YEA293>3.0.CO;2-U

Table S2. Oligonucleotides used for RT-qPCR in this work.

Name	Sequence (from 5' to 3')
FET3-qPCR-F	TGACCGTTTGTCTTCAGGT
FET3-qPCR-R	CTCCACGATTCATCCTTCTC
FTR1-qPCR-F	GGTCACTTGCCTTCACCAA
FTR1-qPCR-R	TTGCTCTTCCGTCAACTCCT
ARN2-qPCR-F	TTCCTTCGCTCCATTCAAG
ARN2-qPCR-R	GAGATAACCCAGCAGCCATT
FIT3-qPCR-F	CATCCTCTAGCACCGCTGAA
FIT3-qPCR-R	CAATAAACATGACGGCAGCAA
FIT1-qPCR-F	TCTAGGGATGCCAATCTGT
FIT1-qPCR-R	ACCAGCGGTAGTGGTTGA
OLE1-qPCR-F	TCGACAAGAAGGGAAACGAA
OLE1-qPCR-R	CATGGTTGTTCGGAGATGTG
ACT1-qPCR-F	TCGTTCCAATTACGCTGGTT
ACT1-qPCR-R	CGGCCAAATCGATTCTCAA
PGK1-qPCR-F	AAGCGTGTCTTCATCAGAGTTG
PGK1-qPCR-R	CGTATCTGGGTGGTGTCC
AFT1-F2	AATGGTGAACGGCGAGTTGAAGTAT GTGAAGCCAGAAGATCGGATCCCC GGGTTAATTAA
AFT1-R1	ATGAAAATGGACGAGAGATACGTC TAAGTTGATTTCATCGAATTGAG CTCGTTAAC
TermTEF:135F	CGACATCATCTGCCAGAT
Aft1+275-R	CAGCCTAATCTACCGGGCAAAA